

Nitrogen cycling in deeply oxygenated sediments: Results in Lake Superior and implications for marine sediments

Jiying Li^{1,*} and Sergei Katsev^{1,2}

¹Large Lakes Observatory, University of Minnesota–Duluth, Duluth, Minnesota

²Department of Physics, University of Minnesota–Duluth, Duluth, Minnesota

Abstract

To understand the nitrogen (N) cycle in sediments with deep oxygen penetration, we measured pore-water profiles to calculate N fluxes and rates at 13 locations in Lake Superior in water depths ranging from 26 to 318 m. Sediments with high oxygen demand, such as in nearshore or high-sedimentation areas, contribute disproportionately to benthic N removal, despite covering only a small portion of the lake floor. These sediments are nitrate sinks (average $0.16 \text{ mmol m}^{-2} \text{ d}^{-1}$) and have denitrification rates (average $0.76 \text{ mmol m}^{-2} \text{ d}^{-1}$) that are comparable to those in coastal marine sediments. The deeply oxygenated (4 to > 12 cm) offshore sediments are nitrate sources (average $0.26 \text{ mmol m}^{-2} \text{ d}^{-1}$) and generate N_2 at lower rates (average $0.10 \text{ mmol m}^{-2} \text{ d}^{-1}$). Ammonium is nitrified with high efficiency (90%), and nitrification supports > 50% of denitrification nearshore and ~ 100% offshore. Oxygen consumption by nitrification accounts for 12% of the total sediment oxygen uptake. About 2% of nitrate reduction is coupled to oxidation of iron, a rarely detected pathway. Our Lake Superior N budget indicates significant contributions from sediment–water exchanges and N_2 production and is closer to balance than previous budgets. Our results reveal that sediment N cycling in large freshwater lakes is similar to that in marine systems. They further suggest that denitrification rates in slowly accumulating, well-oxygenated sediments cannot be described by the same relationship with total oxygen uptake as in high-sedimentation areas; hence, global models should treat abyssal ocean sediments differently than coastal and shelf sediments.

Transformations of nitrogen in aquatic sediments are an important part of the global nitrogen (N) cycle. Sediments actively exchange the reactive nitrogen—nitrate and ammonium—with the water column and contribute to its recycling and removal, accounting for 50–70% of the denitrification in the global ocean (Codispoti et al. 2001). Denitrification (reductive conversion of nitrate to dinitrogen) and nitrification (oxidation of ammonium to nitrate) are the most commonly considered reactions in the sediment nitrogen cycle, though anammox (anaerobic oxidation of ammonium to N_2 with NO_2^- as the electron donor) is increasingly recognized as a significant pathway of nitrogen removal in marine sediments (Dalsgaard et al. 2005). As the reaction rates (Laursen and Seitzinger 2002) and sediment–water exchange fluxes of nitrogen in marine sediments are highly variable (Devol and Christensen 1993), for the purposes of the phenomenological descriptions and global N-cycle modeling sediments are often categorized based on water depth and environment, as follows: estuaries, bays, shelf and coastal oceans, deeper continental margins, and deep oceans (Middelburg et al. 1996; Fennel et al. 2009; Glud et al. 2009). To link the N transformation rates to commonly measured quantities, the rates of nitrification and denitrification have been correlated to sediment oxygen consumption, sedimentation rates, and water depth (Middelburg et al. 1996; Seitzinger et al. 2006). Whereas in marine environments such relationships have been described relatively well, nitrogen cycling in large freshwater lakes has received less attention.

Lake Superior, the world's largest lake by surface area, provides an opportunity to investigate the nitrogen cycle in a freshwater end member system that in many respects is similar to marine systems. Characterized by relatively low organic carbon (C) content (3–5 wt%; Li et al. 2012; Kistner 2013) and slow accumulation rates, the offshore sediments of Lake Superior exhibit an exceptionally deep penetration of oxygen (2 to > 16 cm in water depths between 120 and 300 m; Li et al. 2012), typical of oceanic hemipelagic sediments in 2000–3000 m water depth (Glud 2008). The organic carbon mineralization rates and carbon burial efficiencies in these sediments are similar to those in the deep ocean (Li et al. 2012). The nitrogen dynamics in Lake Superior have been enigmatic (Sterner et al. 2007), as over the last century the lake has experienced an unusual increase in water column nitrate concentrations, leading to an extreme N:P ratio of 10,000 (Guildford and Hecky 2000). The nitrate accumulation has been suggested to result at least partly from the ammonium oxidation in the lake (Finlay et al. 2007), and tentative links to the sediment N cycling have been suggested (Finlay et al. 2013; Small et al. 2013). The sediment's role in the nitrogen cycling in Lake Superior is poorly quantified (Sterner et al. 2007; Li 2011; Small et al. 2013), with scarce geographical coverage and little information available on the rates of critical geochemical pathways, such as nitrification and denitrification. The sediments in Lake Superior exhibit strong temporal and spatial variability, with oxygen penetration varying seasonally by as much as 2 cm (Li et al. 2012), especially at locations with deep oxygen penetration, and with lateral heterogeneity on scales from tens to hundreds of meters (Li et al. 2012). This variability complicates

* Corresponding author: lixx0590@d.umn.edu

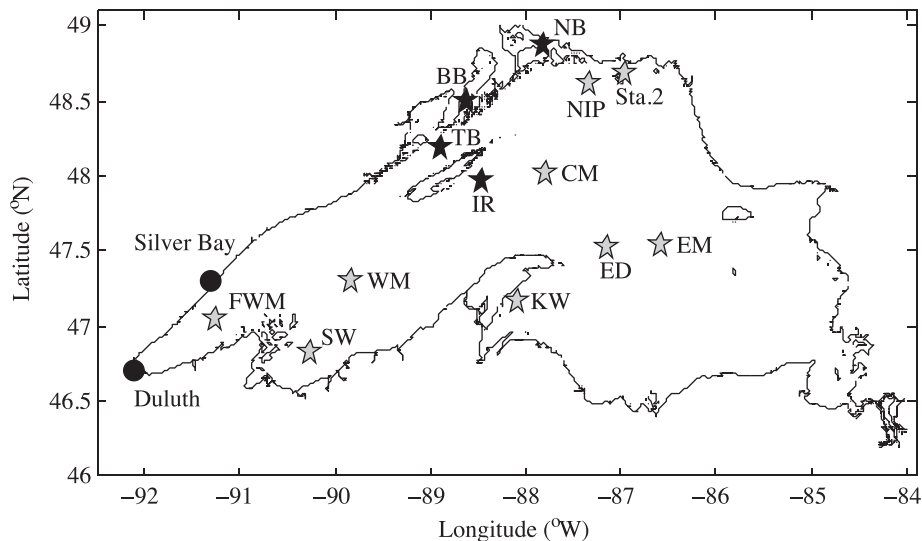


Fig. 1. Sampling locations in Lake Superior. Distances between substations (Table 1) are smaller than the size of the symbol.

comparisons among different sediment cores and necessitates a large number of samplings to obtain representative averages.

In this article, we report the results from a multi-year, multi-season investigation of the sediment nitrogen cycle in Lake Superior. We estimate the nitrate and ammonium fluxes across the sediment–water interface (SWI), calculate the rates of sediment nitrification and denitrification, and discuss the controls on the sedimentary nitrogen cycling in areas of both high and low sedimentation nearshore and offshore. We quantify the sediment contributions to the reactive N recycling in Lake Superior and present an updated geochemical budget for the lake. We further analyze our results to infer the trends in nitrogen cycling across sediments with different sedimentation rates and redox conditions and compare our results to the phenomenological relationships suggested previously for the marine environments.

Methods

Sediment sampling and analyses—Sediments and overlying waters were sampled across Lake Superior on multiple cruises aboard the R/V *Blue Heron* in 2009–2012 (Fig. 1; Table 1) using the procedures described in Li et al. (2012). Briefly, 94 mm internal-diameter sediment cores with undisturbed SWIs were recovered using an Ocean Instruments multi-corer and stored at the in situ temperature of 4°C. Samples of bottom water were collected 2–5 m above the sediment surface using a Rosette Niskin-type sampler. Dissolved oxygen concentrations in sediment pore waters were determined onboard in subsampled thermostated cores, as described previously in Li et al. (2012), using a Unisense (Clark-type) microelectrode. Separate sediment cores from the same multicorer casts were sectioned onboard into 50 mL Falcon tubes in a glove bag under a N₂ atmosphere. Pore waters were immediately extracted from these samples in the N₂-filled glove bag using Rhizon

porous polymer microsamplers (0.1 μm membrane pore size; Dickens et al. 2007). The pore-water samples for nitrate and ammonium analyses were frozen at –18°C until they were measured, and samples for the dissolved Fe(II) analyses were acidified with hydrochloric acid (1% of 6 mol L⁻¹ HCl) immediately after collection and stored at 4°C. Dissolved nitrate concentrations were measured in pore-water and bottom-water samples using the colorimetric method (Grasshoff et al. 1999) on a Lachat Quickchem 8000 flow injection auto-analyzer. Ammonium concentrations were determined by orthophthaldialdehyde (OPA) fluorometry (Holmes et al. 1999). Dissolved Fe(II) concentrations were determined spectrophotometrically with Ferrozine (Viollier et al. 2000). The organic carbon content was measured in freeze-dried sediment by coulometry, as described in Li et al. (2012), on a CM150 total carbon, total organic carbon, total inorganic carbon analyzer. Sediment porosity was determined from measured water content, as described in Li et al. (2012).

Calculations of fluxes and rates—In addition to the diffusive and total oxygen fluxes described in Li et al. (2012), the molecular diffusion fluxes (F_i) of nitrate, ammonium, and dissolved Fe²⁺ were calculated using Fick's law of diffusion:

$$F_i = -\phi D_s \frac{dC_i}{dx} \quad (1)$$

where x is depth below the SWI, C_i is solute concentration (mol per pore-water volume), ϕ is porosity, and $D_s = D/(1 - \phi^2)$ is the appropriate molecular diffusion coefficient corrected for sediment tortuosity (Boudreau 1997). At 4°C, the bulk molecular diffusion coefficients D_i are $D_{O_2} = 438 \text{ cm}^2 \text{ yr}^{-1}$, $D_{NO_3^-} = 349 \text{ cm}^2 \text{ yr}^{-1}$, $D_{NH_4^+} = 352 \text{ cm}^2 \text{ yr}^{-1}$, and $D_{Fe^{2+}} = 123 \text{ cm}^2 \text{ yr}^{-1}$ (Boudreau 1997). Porosity was determined as a function of depth within the sediment, as described in Li et al. (2012). Where concentration gradients near the SWI were poorly resolved, the diffusive fluxes

Table 1. Sampling dates and locations: Far Western Mooring (FWM), Eastern Mooring (EM), Western Mooring (WM), Isle Royale (IR), Central Mooring (CM), Eastern Deep (ED), Keweenaw (KW), Slate Islands (Sta. 2), Southwest (SW), Black Bay (BB), Nipigon Bay (NB), Nipigon Area (NIP), and Thunder Bay (TB). The stations with shallow oxygen penetration (termed “nearshore”) are indicated by †.

Date	Station	Depth (m)	Latitude (N)	Longitude (W)
03 Jun 2009	FWM.1	170	47°02.90'	91°14.97'
10 Nov 2009	FWM.2	160	47°06.26'	91°43.19'
07 Jun 2010	FWM.3	166	47°09.13'	91°16.44'
20 Jul 2010	FWM.4	168	47°02.14'	91°16.38'
21 Sep 2010	FWM.5	166	47°01.98'	91°16.50'
21 Apr 2011	FWM.6	166	47°02.15'	91°16.31'
22 Aug 2011	FWM.7	166	47°02.21'	91°16.32'
05 Jun 2009	EM.1	218	47°32.54'	86°34.31'
06 Oct 2009	EM.2	225	47°32.52'	86°34.31'
10 Jun 2010	EM.3	229	47°33.38'	86°35.76'
22 Jul 2010	EM.4	228	47°33.36'	86°35.65'
22 Sep 2010	EM.5	226	47°33.37'	86°35.68'
26 Jul 2012	EM.6	232	47°32.26'	86°35.79'
04 Jun 2009	WM.1	175	47°18.32'	89°49.43'
04 Oct 2009	WM.2	170	47°18.29'	89°49.73'
11 Jun 2010	WM.3	169	47°19.01'	89°50.73'
22 Jul 2010	WM.4	174	47°18.26'	89°49.33'
25 Sep 2010	WM.5	169	47°19.05'	89°50.76'
23 Apr 2011	WM.6	171	47°19.01'	89°50.80'
08 Jun 2010	†IR.1	234	47°58.41'	88°28.01'
21 Jul 2010	†IR.2	237	47°58.42'	88°28.07'
22 Sep 2010	†IR.3	235	47°58.41'	88°28.08'
21 Apr 2011	†IR.4	235	47°58.40'	88°27.97'
25 Aug 2011	†IR.5	235	47°58.38'	88°28.09'
27 Jul 2012	†IR.6	235	47°58.44'	88°28.05'
08 Jun 2010	CM.1	252	48°01.06'	87°46.44'
21 Jul 2010	CM.2	236	48°02.84'	87°47.32'
22 Sep 2010	CM.3	235	48°02.66'	87°47.17'
22 Apr 2011	CM.4	239	48°03.04'	87°47.74'
21 Jul 2010	ED.1	316	47°31.81'	87°07.81'
22 Sep 2010	ED.2	318	47°31.53'	87°07.49'
22 Apr 2011	ED.3	312	47°31.76'	87°07.65'
09 Jun 2010	KW.1	84	47°09.85'	88°05.32'
04 Jun 2009	Sta. 2	100	48°41.00'	86°57.20'
22 Aug 2011	SW.1	117	46°50.28'	90°16.00'
24 Jul 2012	SW.2	120	46°50.49'	90°16.33'
25 Jul 2012	†BB.1	26	48°30.06'	88°36.48'
25 Jul 2012	†NB.1	29	48°52.46'	88°11.77'
26 Jul 2012	NIP.1	124	48°36.62'	87°20.52'
25 Jul 2012	†TB.1	237	48°11.29'	88°53.04'

across the interface were calculated using the measured pore-water concentrations below the interface, the measured bulk bottom-water concentrations, and a boundary layer thickness of 1 cm (based on the 0.05 cm resolution oxygen profiles; Li 2011; Li et al. 2012). For oxygen fluxes, the contributions from processes other than molecular diffusion, such as bioirrigation (Meile et al. 2005; Glud 2008), were estimated by Li et al. (2012) at 30–50% of the total sediment oxygen uptake. Assuming, for lack of information, a similar effect on the fluxes of other solutes, the total effluxes of NO_3^- and NH_4^+ may be up to 50% higher than the calculated diffusive fluxes. Bioturbation in Lake Superior

is limited to the upper 2 cm of sediment (Li et al. 2012); thus, no contributions from benthic fauna are expected below this depth.

The geochemical reaction rates within the sediment were estimated from the measured vertical concentration profiles using a diagenetic reaction–diffusion equation (Boudreau 1997). At steady state (and neglecting solute advection and bioirrigation), the reaction rates are related to the diffusive transport as

$$0 = \frac{d}{dx} \left(\phi D_s \frac{dC_i}{dx} \right) + \sum_j R_{ij} \quad (2)$$

where R_j are the rates of individual reactions that affect the concentration of solute C_i (Table 2). Using the reaction stoichiometries in Table 2, the rate equations for pore-water nitrate and ammonium, NO_3^- and NH_4^+ , can be written as

$$\frac{d}{dx} \left(\phi D_{s-\text{NO}_3^-} \frac{dC_{\text{NO}_3^-}}{dx} \right) + R_{\text{nitrif.}}(x) - R_{\text{ammonif.}}(x) - R_{\text{denitrif.}}(x) - R_{\text{anammox}}(x) = 0 \quad (3)$$

and

$$\frac{d}{dx} \left(\phi D_{s-\text{NH}_4^+} \frac{dC_{\text{NH}_4^+}}{dx} \right) - R_{\text{nitrif.}}(x) + R_{\text{ammonif.}}(x) - R_{\text{anammox}}(x) + R_{\text{NH}_4^+ \text{ prod.}}(x) = 0 \quad (4)$$

Here, $R_{\text{nitrif.}}$, $R_{\text{ammonif.}}$, $R_{\text{denitrif.}}$, and R_{anammox} are the rates of nitrification, nitrate ammonification (dissimilatory nitrate reduction to ammonium), denitrification, and anammox, respectively, as defined in Table 2. $R_{\text{NH}_4^+ \text{ prod.}}$ is the rate of ammonium production from organic nitrogen during the organic matter mineralization (Table 2).

The rates of nitrification (Table 2) can be obtained in the oxic sediment zone from Eq. 3 by considering that the rates of ammonification, denitrification, and anammox ($R_{\text{ammonif.}}$, $R_{\text{denitrif.}}$, and R_{anammox}) are negligible at high O_2 concentrations ($> 6 \mu\text{mol L}^{-1}$; Seitzinger 1988; Dalsgaard et al. 2005):

$$R_{\text{nitrif.}}(x) = - \frac{d}{dx} \left(\phi D_{s-\text{NO}_3^-} \frac{dC_{\text{NO}_3^-}}{dx} \right) \quad (5)$$

The exceptionally deep oxygenation of sediments in Lake Superior (Li et al. 2012) thus allows the calculation of nitrification rates ($R_{\text{nitrif.}}$) from nitrate concentration profiles (Eq. 5). In surface sediment, where bioirrigation may be important, Eq. 5 should be properly written as

$$R_{\text{nitrif.}}(x) = - \frac{d}{dx} \left(\phi D_{s-\text{NO}_3^-} \frac{dC_{\text{NO}_3^-}}{dx} \right) - \phi \alpha_{\text{irr}} \left(C_{\text{NO}_3^-}^0 - C_{\text{NO}_3^-}^{\text{burr}} \right) \quad (6)$$

where C^0 and C^{burr} are, respectively, the concentrations of nitrate above the sediment surface and within the bioirrigated burrows, and α_{irr} is the bioirrigation coefficient (Katsev et al. 2007). For a typical concentration gradient

Table 2. Major reactions affecting nitrogen cycling in sediments.

Processes		Rate
Aerobic respiration	$(\text{CH}_2\text{O})_x(\text{NH}_3)_y + x \text{O}_2 \rightarrow x \text{CO}_2 + y \text{NH}_3 + x \text{H}_2\text{O}$	$R_C = -x/y R_{\text{NH}_4^+ \text{ prod.}}$
Denitrification	$(\text{CH}_2\text{O})_x(\text{NH}_3)_y + 4x/5 \text{NO}_3^- \rightarrow x/5 \text{CO}_2 + 4x/5 \text{HCO}_3^- + 2x/5 \text{N}_2 + y \text{NH}_3 + x \text{H}_2\text{O}$	$R_C = 5/4 R_{\text{denitrif.}}$
Nitrification	$\text{NH}_4^+ + 2 \text{O}_2 + 2 \text{HCO}_3^- \rightarrow \text{NO}_3^- + 2 \text{CO}_2 + 3 \text{H}_2\text{O}$	$R_{\text{nitrif.}}$
Nitrate ammonification ¹	$\text{NO}_3^- + 8 e^- + 7 \text{H}_2\text{O} \rightarrow \text{NH}_4^+ + 10 \text{OH}^-$	$R_{\text{ammonif.}}$
Anammox	$\text{NH}_4^+ + \text{NO}_3^- \rightarrow \text{N}_2 + 2 \text{H}_2\text{O}$	R_{anammox}
Anaerobic Fe oxidation	$\text{Fe}^{2+} + \frac{1}{8} \text{NO}_3^- + \frac{7}{8} \text{H}_2\text{O} + \frac{7}{4} \text{OH}^- \rightarrow \frac{1}{8} \text{NH}_4^+ + \text{Fe}(\text{OH})_3$	$R_{\text{Fe}^{2+} \text{ oxidation}}$

¹ The listed half-reaction may be coupled with the oxidation of organic C, reduced Fe, or sulfur (S) (Hulth et al. 2005).

for nitrate in Lake Superior ($C^0 - C^{\text{bur}} < 0$, see below), Eq. 5 yields the minimum nitrification rates, and the actual rates could be higher. The area-specific (integrated over the sediment depth) nitrification rates ($\text{mmol m}^{-2} \text{d}^{-1}$) can be calculated by integrating Eq. 5 from the SWI ($x = 0$) into the bottom of the nitrification zone L :

$$\begin{aligned}
 R_{\text{nitrif.}}^* &= \int_0^L R_{\text{nitrif.}}(x) dx = - \int_0^L \frac{d}{dx} \left(\varphi D_{\text{s-NO}_3^-} \frac{dC_{\text{NO}_3^-}}{dx} \right) dx \\
 &= \left(\varphi D_{\text{s-NO}_3^-} \frac{dC_{\text{NO}_3^-}}{dx} \right)_{x=0} - \left(\varphi D_{\text{s-NO}_3^-} \frac{dC_{\text{NO}_3^-}}{dx} \right)_{x=L} \quad (7) \\
 &= F_{\text{NO}_3^-}(x=L) - F_{\text{NO}_3^-}(x=0)
 \end{aligned}$$

Here, $R_{\text{nitrif.}}^*$ is the depth-integrated nitrification rate, and $F_{\text{NO}_3^-}(x=0)$ and $F_{\text{NO}_3^-}(x=L)$ are the diffusive fluxes at the SWI and $x = L$, respectively. The depth L can be chosen at the depth within the oxygenated zone where $F_{\text{NO}_3^-}$ reaches a maximum (see Results for details).

The pore-water nitrate can be removed through denitrification, anammox, or the dissimilatory nitrate reduction (DNR) to ammonium (ammonification; Table 2; Hulth et al. 2005). The net rate of nitrate consumption, $-\sum R_{\text{NO}_3^-}$, by all three of these pathways can be described at steady state, and neglecting bioirrigation (Eq. 2), as

$$\sum R_{\text{NO}_3^-}(x) = - \frac{dF_{\text{NO}_3^-}}{dx} = \frac{d}{dx} \left(\varphi D_{\text{s-NO}_3^-} \frac{dC_{\text{NO}_3^-}}{dx} \right) \quad (8)$$

where $F_{\text{NO}_3^-}$ is the vertical flux of nitrate. By integrating Eq. 8 from L , the upper boundary of the zone of net nitrate reduction, to L^∞ , the depth at which the nitrate gradients vanish, the depth-integrated rates of net nitrate consumption ($R_{\text{NO}_3^- \text{ cons.}}^*$) can be expressed as

$$\begin{aligned}
 R_{\text{NO}_3^- \text{ cons.}}^* &= - \int_L^{L^\infty} R_{\text{NO}_3^-}(x) dx \\
 &= \left(\varphi D_{\text{s-NO}_3^-} \frac{dC_{\text{NO}_3^-}}{dx} \right) \Big|_{x=L}^{x=L^\infty} \quad (9) \\
 &= F_{\text{NO}_3^-}(x=L)
 \end{aligned}$$

where $F_{\text{NO}_3^-}(x=L)$ is the diffusive flux at L (i.e., the maximum downward flux; see below for details).

The rates of reactive nitrogen removal to N_2 by denitrification and anammox (Table 2) can be calculated by neglecting nitrification in anoxic sediment. Denitrification is typically the dominant pathway of nitrogen removal in freshwater (Hulth et al. 2005), but anammox was recently also found to be significant (Schubert et al. 2006; Zhu et al. 2013), including in Lake Superior (S. A. Crowe unpubl.), so anammox cannot be a priori neglected. By rearranging Eqs. 3 and 4, we obtain

$$\begin{aligned}
 R_{\text{N removal}} &= R_{\text{denitrif.}}(x) + 2R_{\text{anammox}}(x) \\
 &= \frac{d}{dx} \left(\varphi D_{\text{s-NH}_4^+} \frac{dC_{\text{NH}_4^+}}{dx} \right) + \\
 &\quad \frac{d}{dx} \left(\varphi D_{\text{s-NO}_3^-} \frac{dC_{\text{NO}_3^-}}{dx} \right) - R_{\text{NH}_4^+ \text{ prod.}}(x) \quad (10)
 \end{aligned}$$

Here, $R_{\text{NH}_4^+ \text{ prod.}}$ is the rate of ammonium production from organic nitrogen during organic matter mineralization. To calculate the area-specific rates of nitrogen removal, we integrate Eq. 10 from SWI ($x = 0$) to some maximum depth L^∞ at which the concentrations of NO_3^- and NH_4^+ no longer vary with depth and at which their diffusive fluxes are negligible. The total nitrogen removal rate (Eq. 11) then can be calculated as a difference between the total ammonium production within the sediment and the NO_3^- and NH_4^+ fluxes out (negative) of the sediment:

$$\begin{aligned}
 R_{\text{N removal}}^* &= - \int_0^{L^\infty} R_{\text{denitrif.}}(x) dx \\
 &\quad + 2 \int_0^{L^\infty} R_{\text{anammox}}(x) dx \\
 &= \left(\varphi D_{\text{s-NH}_4^+} \frac{dC_{\text{NH}_4^+}}{dx} \right) \Big|_{x=0}^{x=L^\infty} \\
 &\quad + \left(\varphi D_{\text{s-NO}_3^-} \frac{dC_{\text{NO}_3^-}}{dx} \right) \Big|_{x=0}^{x=L^\infty} \quad (11) \\
 &\quad + \int_0^{L^\infty} R_{\text{NH}_4^+ \text{ prod.}}(x) dx \\
 &= F_{\text{NO}_3^-}(x=0) \\
 &\quad + F_{\text{NH}_4^+}(x=0) + \frac{1}{12} R_C^*
 \end{aligned}$$

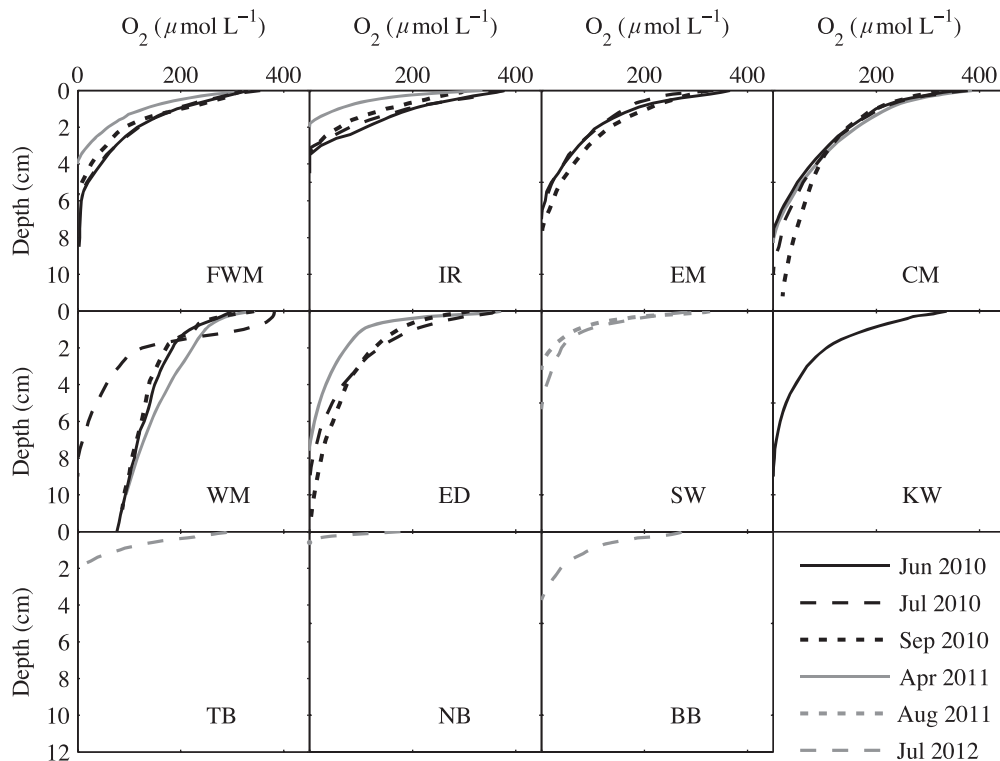


Fig. 2. Vertical distributions of dissolved oxygen in sediment pore waters in June, July, and September of 2010; April and August 2011; and July 2012. The 2010 data for the offshore stations are re-plotted from Li et al. (2012).

The last term in Eq. 11 describes the production of ammonium from organic N, based on the C mineralization rate, R_C^* (Li et al. 2012) and the C:N ratio of 12:1 in Lake Superior (Heinen and McManus 2004; Sterner et al. 2008). In N-rich Lake Superior, the variation in the C:N ratio with depth in the sediment does not exhibit a clear pattern (Ostrom et al. 1998).

Results

Oxygen penetration at sites with high vs. low sedimentation—In contrast to the previously investigated (Li et al. 2012) open-water locations in which oxygen penetrated deeply into the sediments (4 to > 12 cm, Fig. 2), the oxygen penetration depths (OPDs) in the enclosed bays and other locations with high sedimentation (e.g., Sta. Thunder Bay [TB], Black Bay [BB], Nipigon Bay [NB]; sedimentation rates presented in Li et al. [2012] and Kistner [2013]) were shallower, from 0.5 to 3 cm (Figs. 1, 2). These sediments are characterized by higher oxygen uptake rates (Tables 3 and 4), though not necessarily by higher organic carbon contents on a wt% basis (Kistner 2013). In addition to the bay and nearshore areas, such sediments can be found in the high-sedimentation areas (Li 2011) in the deep water, sometimes at significant distances from shores (Table 1; Fig. 1). In analogy to marine systems, where coastal sediments typically have higher sedimentation rates and greater oxygen uptakes than do pelagic sediments, we will refer to such sediments as “nearshore,” for convenience, in contrast to the “offshore” sites with deep OPDs.

Pore-water nitrate, ammonium, and dissolved Fe(II)—The pore-water nitrate distributions (Fig. 3) at sites with deep OPDs exhibit peaks several millimeters below the sediment–water interface, a common feature in carbon-poor sediments (Coloway and Bender 1982; Burdige 2006) resulting from aerobic oxidation of ammonium (Middelburg et al. 1996). The resultant increased concentrations in the surface sediments compared to the overlying waters indicate the diffusive fluxes of nitrate from sediments into the water column (Eq. 1). The nitrate concentrations below the peaks decrease into the anoxic sediment, indicating nitrate reduction (Table 2). Nitrate is typically exhausted within several centimeters of the OPD (Fig. 3). In sediments with deep oxygen penetrations (e.g., > 10 cm at Sta. Eastern Mooring [EM] and Western Mooring [WM]), the nitrate penetrations are also deep; in sediments with shallow OPDs (e.g., Sta. Isle Royale [IR], NB, BB, and TB), the nitrate penetrations are shallow, typically less than 4 cm (Fig. 3). The nitrate concentrations at Sta. TB were negligible below the SWI (not shown), despite the $28.7 \mu\text{mol L}^{-1}$ concentration in the overlying water column. The concentrations of ammonium, which is produced during organic matter mineralization, increase with depth within the sediment at all stations (Fig. 4). The ammonium concentration gradients at the SWI indicate effluxes into the water column. The nitrate and ammonium profiles (Figs. 3, 4) exhibit high variability among samplings, consistent with the heterogeneity of the sediments (Li et al. 2012). Though this variability precluded the detection of seasonal trends, the large number of profiles

Table 3. The diffusive fluxes of nitrate ($F_{\text{NO}_3^-}$) and ammonium ($F_{\text{NH}_4^+}$) across the sediment–water interface (positive into the sediment), the depth-integrated rates of nitrification ($R_{\text{nitrif.}}^*$), the fraction of the total oxygen uptake (TOU; see Table 4) consumed by nitrification ($R_{\text{nitrif.}}^*/\text{TOU}$), the integrated rates of nitrate consumption by denitrification and other pathways ($R_{\text{NO}_3^- \text{ cons.}}^*$), and the contribution of Fe oxidation ($R_{\text{Fe}^{2+}}^*$) to nitrate reduction. The stations with shallow oxygen penetration (termed “nearshore”) are indicated by †. All fluxes and integrated rates are in $\text{mmol m}^{-2} \text{d}^{-1}$.

Station	$F_{\text{NO}_3^-}$	$F_{\text{NH}_4^+}$	$R_{\text{nitrif.}}^*$	$R_{\text{nitrif.}}^*/\text{TOU}$ (%)	$R_{\text{NO}_3^- \text{ cons.}}^*$	$R_{\text{nitrif.}}^*$: $R_{\text{NO}_3^- \text{ cons.}}^*$ (%)	$R_{\text{Fe}^{2+}}^*$	$R_{\text{NO}_3^- \text{ cons.}}^*$ (%)	$R_{\text{Fe}^{2+}}^*$: $R_{\text{NO}_3^- \text{ cons.}}^*$ (%)
FWM.1	-0.11	-0.0091	0.21		0.085				
FWM.3	-0.23	-0.017	0.39		0.15				
FWM.4	-0.34		0.44		0.084				
FWM.5	-0.17; -0.29	0							
FWM.6	-0.13; -0.10		0.27		0.088; 0.086				
FWM.7	-0.10; -0.23		0.21; 0.29; 0.27	8.4	0.092; 0.074; 0.061				
Average	-0.19±0.09	-0.0087±0.0085	0.28±0.09		0.090±0.03	32			
EM.1	-0.15	-0.024							
EM.2	-0.27		0.39; 0.37		0.11; 0.091				
EM.3	-0.36	-0.13	0.51		0.14		0.0009		0.8
EM.4	-0.20	-0.091	0.48		0.28				
EM.5	-0.12; -0.16	-0.0087; -0.018	0.23; 0.31		0.034; 0.040		0.0022		5.5
EM.6	-0.13	-0.029	0.29		0.15				
Average	-0.20±0.09	-0.050±0.049	0.37±0.10	8.9	0.12±0.08	32			
WM.1	-0.19	-0.020	0.33						
WM.2	-0.28		0.35						
WM.3	-0.37	-0.11	0.56						
WM.4	-0.17	-0.045; -0.022	0.21		0.036		0.0007		1.9
WM.5	-0.17; -0.20		0.33						
Average	-0.23±0.08	-0.049±0.04	0.36±0.08	16	0.036±0.015	10			
CM.1	-0.23	-0.019	0.29		0.049				
CM.2	-0.24	-0.11	0.29		0.036				
CM.3	-0.20		0.39; 0.26; 0.39		0.046; 0.087				
CM.4	-0.22		0.33; 0.35		0.096; 0.060				
Average	-0.22±0.02	-0.065±0.06	0.32±0.05		0.066±0.024	21	0.0012		1.5
†IR.1	-0.09	-0.034	0.21		0.11				
†IR.2	-0.32		0.53		0.21				
†IR.3	-0.13; -0.15	0	0.36; 0.34; 0.36		0.14; 0.12; 0.14				
†IR.4	-0.92; -0.54								
†IR.5	-0.07								
†IR.6	-0.91; -0.31		0.25		0.13				
Average	-0.38±0.29	-0.017	0.74		0.42				
ED.1	-0.44	-0.10; -0.061	0.40±0.18	16	0.18±0.11	45			
ED.2	-0.11		0.63		0.17				
ED.3	-0.17; -0.44		0.18; 0.22		0.079; 0.061				
Average	-0.29±0.17	-0.081±0.027	0.21		0.045		0.0005		1.1
SW.1	-0.15		0.37±0.20	9.6	0.087±0.055	28			
SW.2	-0.15; -0.58	-0.025	0.23; 0.27		0.066; 0.11		0.0004		0.9
Average	-0.29±0.15	-0.030	0.61				0.0032		3.7
KW.1	-0.33	-0.036	0.37±0.16		0.088	24			
Sta.2	-0.31	-0.036	0.36		0.032	8.8	0.0006		1.9
†TB.1	0.52	-0.029							
NIP.1	-0.27	-0.015	0.62						
†NB.1	-0.076	-0.044	0.32		0.24	76			
†BB.1	0.047	-0.029	0.13		0.17	131			

Table 4. The rates of nitrogen removal to N_2 by denitrification and anammox ($R_{N\text{ removal}}^*$; Eq. 11). The stations with shallow oxygen penetration (termed “nearshore”) are indicated by †. The measured total oxygen uptakes (TOU) are from Li et al. (2012). For other locations (indicated by *), to account for bioirrigation, the total fluxes of NO_3^- , NH_4^+ , and O_2 were increased by 50% compared to diffusive fluxes.

	Oxygen diffusive fluxes ($mmol\ m^{-2}\ d^{-1}$)	Total oxygen uptake, TOU ($mmol\ m^{-2}\ d^{-1}$)	Nitrogen removal to N_2 ($mmol\ m^{-2}\ d^{-1}$)	Organic C mineralized by denitrification (%)
FWM	3.0 (1.1–7.8)	6.7	0.19 ± 0.01	<4
EM	2.9 (1.3–4.6)	4.4*	0.031 ± 0.06	<2
WM	2.2 (1.1–3.2)	4.4	0.029 ± 0.024	<2
CM	3.2 (2.3–3.8)	4.8*	<0.035	<1
†IR	5.0 (2.7–7.3)	4.9	0.26 ± 0.05	<8
ED	4.2 (2.7–6.8)	6.3*	<0.049	<1
SW	4.9 (3.9–6.5)	7.4*	0.25 ± 0.03	<5
†TB	5.1 (4.4, 5.8)	7.7*	1.4 ± 0.1	<31
†BB	7.1 (8.7, 5.4)	11*	0.84 ± 0.06	<16
†NB	6.4 (6.8, 5.9)	10*	0.54 ± 0.04	<12

allowed the calculation of the average fluxes and rates (Table 3). The concentrations of dissolved Fe^{2+} (Fig. 5) increase with depth below the OPD, suggesting iron reduction in the anoxic sediment and Fe^{2+} oxidation near the depth of oxygen penetration. In Lake Superior, prominent iron- and manganese-rich sediment layers that result from metal oxidation are often visible to the naked eye (optical images and scanning X-ray fluorescence profiles are presented in Li [2011] and Li et al. [2012]). In cores in which nitrate penetrated significantly below the OPD, Fe^{2+} appears in pore waters below the depth of nitrate penetration.

Nitrate and ammonium fluxes across the sediment–water interface—Sediments at the sites with deep penetration of nitrate (> 3 cm; Fig. 3; Sta. Far Western Mooring [FWM], EM, WM, Central Mooring [CM], East Deep [ED], Southwest [SW], Keweenaw [KW], Nipigon Area [NIP]) were sources of nitrate to the overlying waters, with diffusive effluxes that ranged from 0.19 to $0.33\ mmol\ m^{-2}\ d^{-1}$ (Table 3). At Sta. NB, where nitrate was depleted within 1 cm of the sediment surface, the efflux was significantly lower, $0.076\ mmol\ m^{-2}\ d^{-1}$. At the enclosed-bay sites Sta. TB and BB, the diffusive fluxes were into the sediment, at 0.52 and $0.047\ mmol\ m^{-2}\ d^{-1}$,

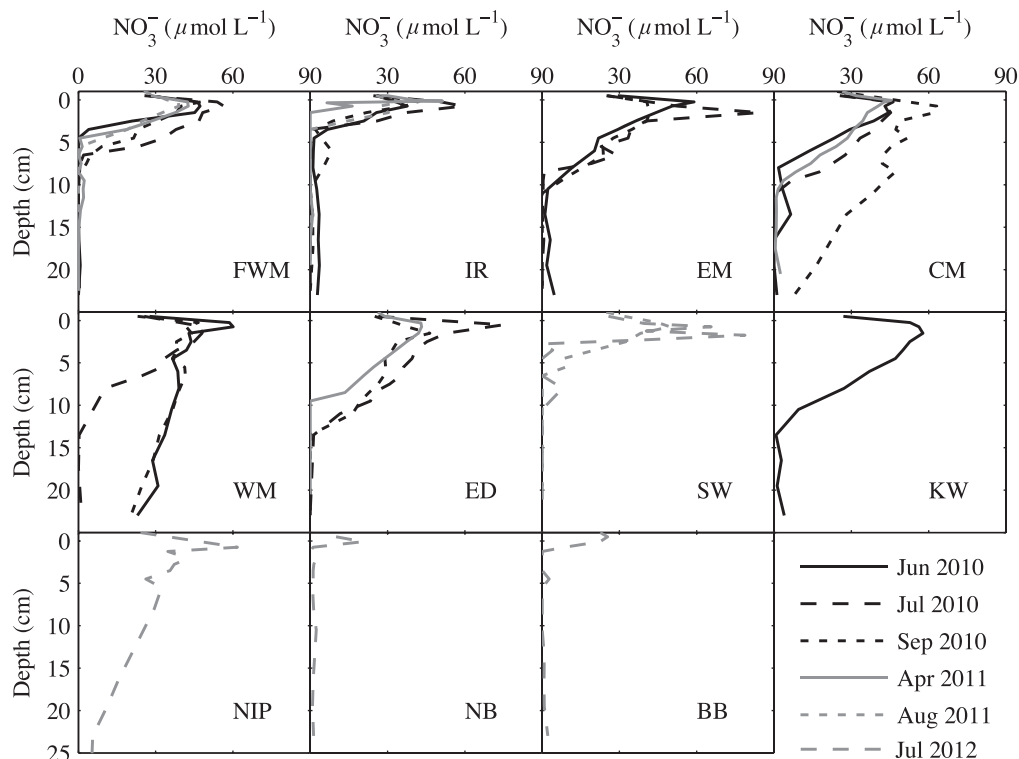


Fig. 3. Vertical distributions of pore-water nitrate in June, July, and September 2010; April and August 2011; and July 2012.

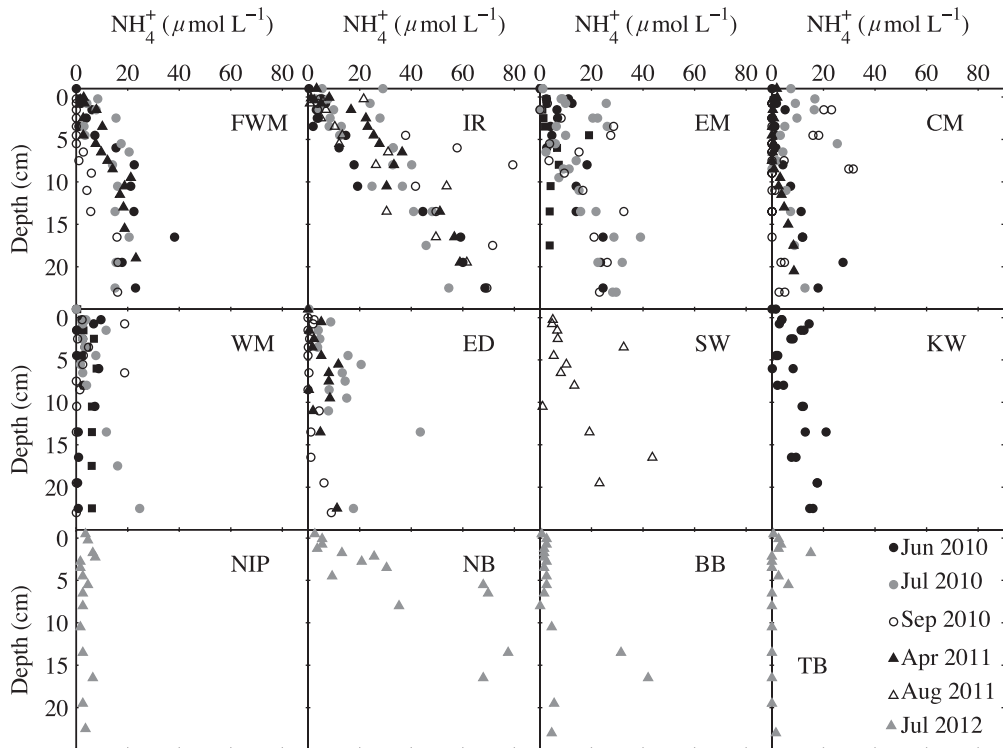


Fig. 4. Vertical distributions of pore-water ammonium in June 2009; June, July, and September 2010; April and August 2011; and July 2012.

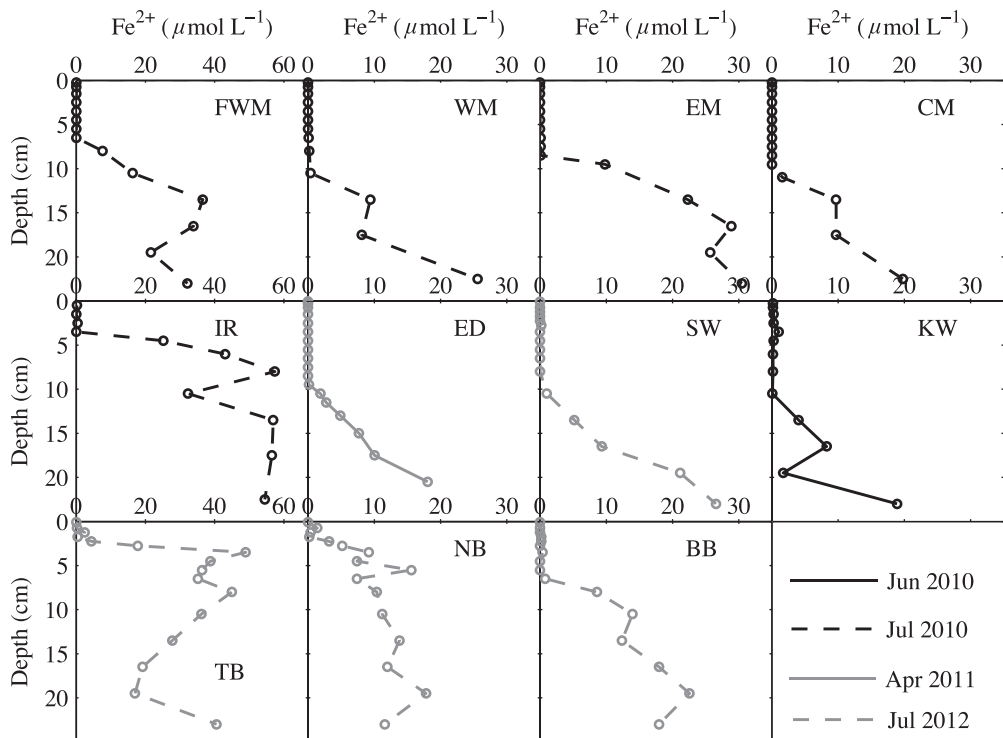


Fig. 5. Typical profiles of dissolved Fe(II) in sediments of Lake Superior. The data (see Table 1) are for June, July 2010, April 2011, and July 2012.

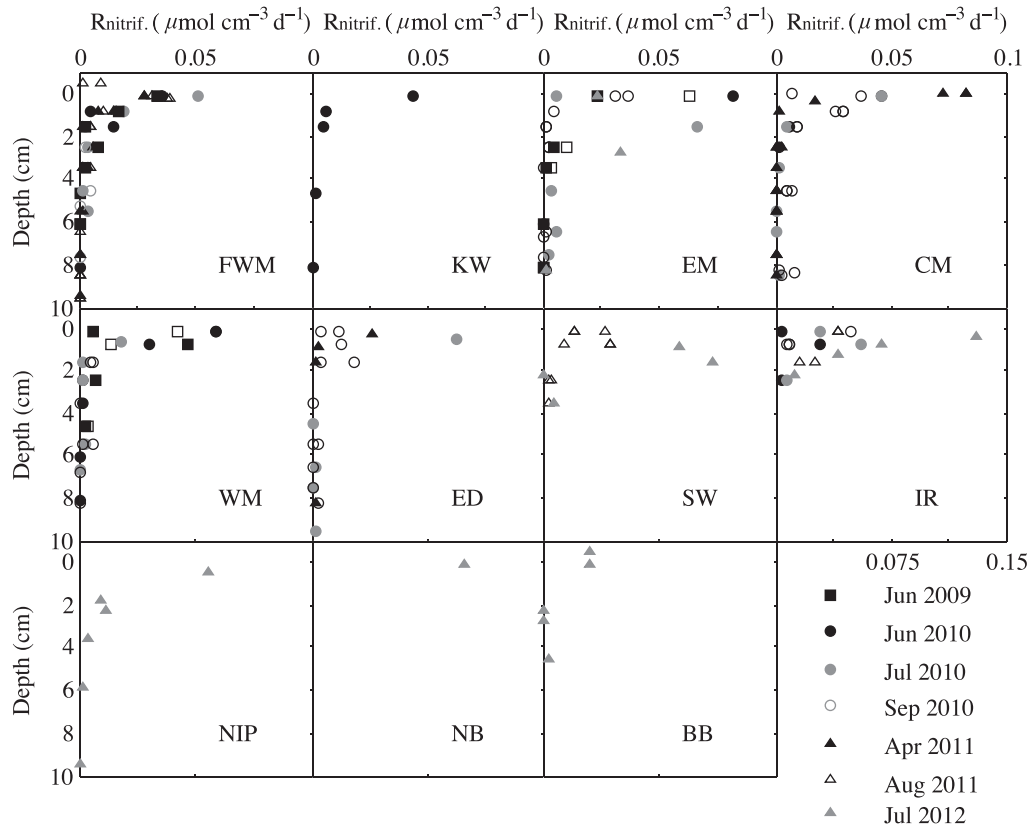


Fig. 6. Calculated rates of sediment nitrification. The data are for June and October 2009; June, July, and September 2010; April and August 2011; and July 2012.

respectively. The effluxes of ammonium were small at all stations ($0.0087\text{--}0.081\text{ mmol m}^{-2}\text{ d}^{-1}$; Table 3). Bioirrigation is expected to affect the nitrate and ammonium fluxes to a lesser degree than it does oxygen fluxes (30–50%; Li et al. 2012), as the bioirrigation coefficients for nitrate and ammonium are lower (Meile et al. 2005) and the respective concentration gradients are weaker.

Nitrification rates—The calculated nitrification rates (Fig. 6) indicated active nitrification in the upper 4 cm of sediment. The rates peaked 0.5–1.5 cm below the sediment–water interface independent of the oxygen penetration depth. The maximum rates varied between 0.02 and $0.15\ \mu\text{mol cm}^{-3}\text{ d}^{-1}$ (Fig. 6). The nitrification rates decreased below 2 cm and became negligible below 4 cm at all locations. The depth-integrated nitrification rates (Table 3) ranged between 0.21 and $0.74\text{ mmol m}^{-2}\text{ d}^{-1}$ (average $0.35\text{ mmol m}^{-2}\text{ d}^{-1}$). The effect of bioirrigation on these integrated rates can be estimated by integrating the bioirrigation term in Eq. 6 over the bioturbated upper 2 cm of sediment. For a typical bioirrigation coefficient of $\alpha_{\text{irr}} < 10^{-6}\text{ s}^{-1}$ (Matisoff and Wang 1998) and the nitrate concentration gradient of $C^0 - C^{\text{bur}} < 30\ \mu\text{mol L}^{-1}$ (Fig. 3), bioirrigation should increase the nitrification rate by less than $0.05\text{ mmol m}^{-2}\text{ d}^{-1}$, which is within the uncertainty (Table 3).

Nitrate reduction rates—Nitrate reduction (by denitrification, anammox, and dissimilatory nitrate reduction to

ammonium; Fig. 7) typically occurred 2–5 cm below the sediment surface in the high-sedimentation regions and below 3–7 cm in the low-sedimentation regions, within several centimeters of the OPD. Figure 7 shows the calculated vertical fluxes of nitrate, $F_{\text{NO}_3^-}$, and the net nitrate consumption rates $-\sum R_{\text{NO}_3^-}$ (Eq. 8) in two typical sediments. As the upper boundary of the nitrate reduction zone (L in Eq. 9) is below the bioturbation zone (Fig. 7), the calculated nitrate reduction rates are essentially unaffected by bioturbation and bioirrigation. The depth-integrated rates of nitrate consumption (Eq. 9) range between 0.032 and $0.24\text{ mmol m}^{-2}\text{ d}^{-1}$ (Table 3). They are lower in sediments with deep oxygen penetrations ($0.032\text{--}0.12\text{ mmol m}^{-2}\text{ d}^{-1}$ at Sta. FWM, EM, WM, CM, KW, and ED; average $0.080\text{ mmol m}^{-2}\text{ d}^{-1}$) and higher in sediments with shallower OPDs ($0.18\text{--}0.24\text{ mmol m}^{-2}\text{ d}^{-1}$ at Sta. IR, NB, and BB; average $0.20\text{ mmol m}^{-2}\text{ d}^{-1}$).

N_2 production rates—The calculated rates of N_2 production by denitrification and anammox (Table 2; Eq. 11) are presented in Table 4. At deeply oxygenated sites (Sta. EM, WM, CM, ED), the rates are small ($< 0.05\text{ mmol m}^{-2}\text{ d}^{-1}$). For example, at these rates, denitrification would account for less than 5% of the total organic carbon mineralization. In contrast, at the high-sedimentation sites with shallower OPDs (Sta. TB, BB, NB), the rates of the reactive nitrogen removal to N_2 (Eq. 11) are an order of magnitude higher ($> 0.5\text{ mmol m}^{-2}\text{ d}^{-1}$; Table 4). Denitrification at these rates would account for 12–31% of the total carbon mineralization.

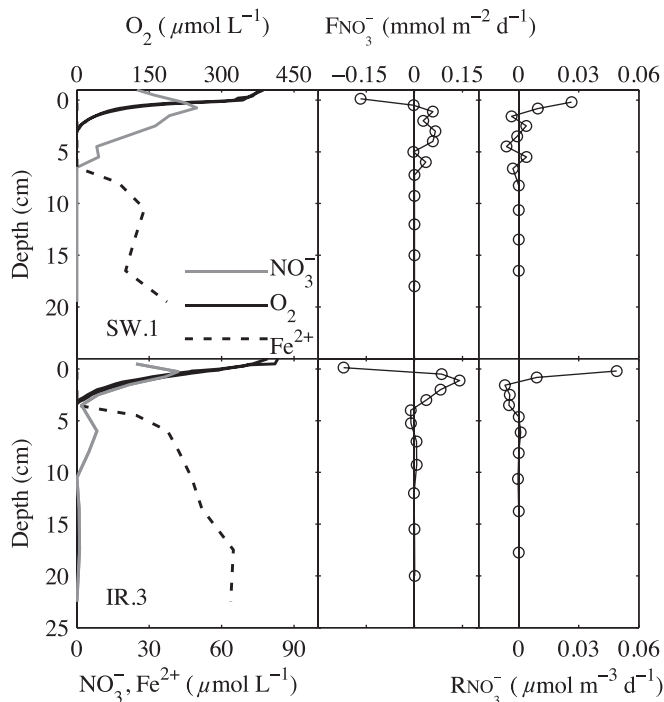


Fig. 7. Typical distributions of dissolved Fe^{2+} , O_2 , and NO_3^- , the corresponding nitrate fluxes, $F_{\text{NO}_3^-}$ (negative if into the water column; Table 3), and the corresponding nitrate consumption rates $R_{\text{NO}_3^-}$ (positive for nitrate production). The depth L where $R_{\text{NO}_3^-}$ falls to zero and $F_{\text{NO}_3^-}$ reaches maximum separates the zones of net nitrate production (above) and consumption (below).

The calculated rates of N_2 production in Table 4 are only weakly sensitive to bioirrigation: based on Eq. 11, a conservatively estimated 100% uncertainty in the total fluxes of NO_3^- , NH_4^+ , and O_2 translates into a 30% uncertainty in the depth-integrated rates.

Discussion

The reactions in the sediment nitrogen cycle are tightly coupled (Table 2). Organic matter mineralization mobilizes organic N as ammonium, which subsequently can be oxidized to either nitrate (nitrification) or N_2 (anammox). The produced nitrate is used in denitrification to oxidize organic carbon and is reduced in the process to N_2 (Hulth et al. 2005). The pore-water nitrate and ammonium may be exchanged with the water column, thus recycling the reactive nitrogen into the ecosystem, whereas the unmineralized fraction of organic nitrogen may be buried into the deep sediment. Below we analyze these processes in more detail, identify the trends in their rates, and use them to compile geochemical budgets.

Nitrification—Nitrification is a major biogeochemical pathway that transforms ammonium to nitrate. In addition to the calculation method based on our Eq. 7, the gross rate of ammonium production can be estimated from the total sediment oxygen uptake ($\sim 6.7 \text{ mmol m}^{-2} \text{ d}^{-1}$ offshore; Li et al. 2012). As 1 mol of O_2 is needed to oxidize 1 mol of

organic carbon and 2 mols of O_2 are needed to oxidize 1 mol of NH_4^+ (Table 2), the 12 C:1 N:14 O_2 stoichiometry of the organic matter oxidation leads to a gross ammonium production rate of approximately $6.7/14 = 0.48 \text{ mmol m}^{-2} \text{ d}^{-1}$. Subtracting the previously calculated average efflux of ammonium ($0.045 \text{ mmol m}^{-2} \text{ d}^{-1}$; Table 3) yields an ammonium oxidation rate that closely matches the nitrification rates calculated from Eq. 5 ($0.28\text{--}0.40 \text{ mmol m}^{-2} \text{ d}^{-1}$; Table 3). These in situ rates are about an order of magnitude lower than the potential rates (Small et al. 2013) determined in sediment slurries amended with ammonium ($1.5\text{--}6.5 \text{ mmol m}^{-2} \text{ d}^{-1}$ nearshore and $38 \text{ mmol m}^{-2} \text{ d}^{-1}$ offshore; Stark 2009). The mismatch suggests that in the well-oxygenated sediments of Lake Superior nitrification is limited by the availability of ammonium (Rysgaard et al. 1994); thus, the potential rates may greatly exceed the in situ rates.

The efficiency of ammonium oxidation is high: a ratio of the ammonium efflux to ammonium production yields $1 - (0.045/0.48) = 90\%$. Despite this, in Lake Superior, nitrification accounts for only 9–16% (average 12%) of the total sediment oxygen uptake (Table 3), which is a noticeably smaller fraction than in marine sediments: 35% in the coastal regions (Seitzinger et al. 1984), 21% on the continental shelf (Laursen and Seitzinger 2002), and 21–45% on the continental slope and abyssal plains (Christensen and Rowe 1984). The reason seems to be the higher C:N ratio in the organic material in Lake Superior (11 to 13; Heinen and McManus 2004; Sterner et al. 2008). For the organic matter oxidation stoichiometry above, a complete oxidation of the produced ammonium should consume $2 \times 1/(12 + 2) = 14\%$ of the total O_2 flux (which matches our result), as opposed to 23% for the Redfield ratio of 6.6.

Nitrate reduction and N_2 production—Sediment nitrate can be removed through denitrification, anammox, or DNR to ammonium (ammonification; Table 2; Hulth et al. 2005). Ammonification recycles nitrate to ammonium, whereas denitrification and anammox remove the reactive nitrogen from the system by converting it to N_2 . The calculated nitrate reduction rates (Table 3) indicate that in Lake Superior these processes remove between 9% and 100% of the nitrate produced by nitrification. The rest escapes the sediment in the form of nitrate effluxes, which are significantly higher in the deeply oxygenated offshore sediments (Table 3), where they remove between 44% and 91% of the produced nitrate. Accordingly, the efficiency of nitrate removal is lower at the sites with deep OPDs (e.g., 8.8% at Sta. KW and 32% at Sta. FWM and EM) and higher at sites with shallower OPDs (45% at Sta. IR, 76% at Sta. NB, and 100% at Sta. BB). Similarly, the overall rates of N_2 production by denitrification and anammox are higher in sediments characterized by high sedimentation and shallow oxygen penetrations, such as the nearshore sites Sta. BB, NB, TB, and IR ($0.26\text{--}1.4$, average $0.76 \text{ mmol m}^{-2} \text{ d}^{-1}$; Table 4), than in sediments at the low-sedimentation offshore sites ($0.029\text{--}0.25$, average $0.10 \text{ mmol m}^{-2} \text{ d}^{-1}$). These calculated rates of N_2 production are similar to the ones reported in Lake

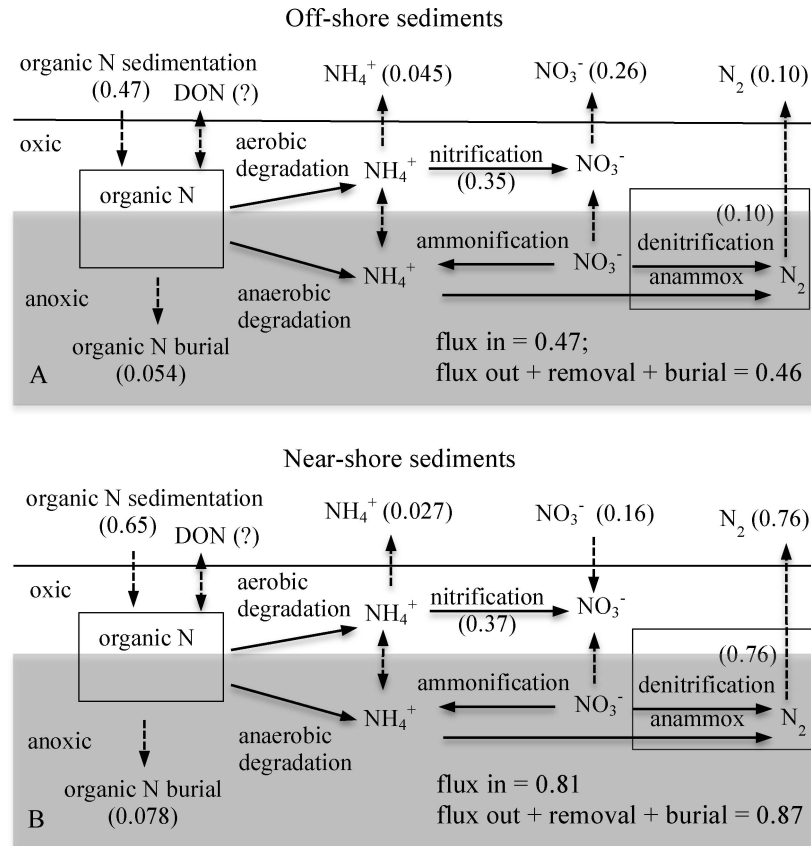


Fig. 8. Nitrogen cycling in Lake Superior sediments: (A) in low-sedimentation areas with deep oxygen penetration (Sta. FWM, EM, WM, CM, SW, ED, NIP); (B) in high-sedimentation areas with shallow oxygen penetrations (Sta. IR, TB, BB, NB). All fluxes and integrated rates are in $\text{mmol N m}^{-2} \text{d}^{-1}$. Horizontal solid lines indicate the SWI; solid arrows indicate diagenetic reactions; dashed arrows indicate sedimentation and diffusion fluxes. The values are averages from Tables 3 and 4. The organic nitrogen fluxes are discussed in the text.

Superior by Small et al. (2013). At high-sedimentation sites, the nitrate for denitrification (and anammox) is supplied by both nitrification (average about 50%; Tables 3, 4) and the nitrate fluxes (50%) from the water column (average $0.16 \text{ mmol m}^{-2} \text{d}^{-1}$). At the low-sedimentation offshore sites, nitrification in the oxic sediment layer is the only source of nitrate for the deeper anoxic sediment and thus an important control on the rates of reactive nitrogen removal. This parallels the situation in marine sediments (Seitzinger 1988), where nitrification supports between 60% and 100% of the total denitrification in the continental shelf sediments (Devol et al. 1997; Laursen and Seitzinger 2002).

Nitrate reduction coupled to iron oxidation—Studies have suggested that nitrate reduction may be coupled to the oxidation of reduced Fe (Straub and Buchholz-Cleven 1996; Benz et al. 1998): in pelagic marine sediments, ferrous iron (Fe^{2+}) often appears in pore water only below the depth of nitrate penetration (Burdige 1993). At several of our sites, the depth of iron oxidation coincided with the penetration depth of nitrate (NPD) rather than of oxygen. At Sta. EM, CM, and SW, nitrate penetrated 3 cm deeper than oxygen, and Fe^{2+} appeared only below the depth of

nitrate penetration (Figs. 5, 7). This suggests that in Lake Superior nitrate reduction is at least partially coupled to Fe^{2+} oxidation. The depth-integrated iron oxidation rates can be estimated from the Fe^{2+} fluxes immediately below the oxidation depth (L'):

$$R_{\text{Fe}^{2+} \text{ oxidation}}^* = - \left(\phi D_{s-\text{Fe}^{2+}} \frac{dC_{\text{Fe}^{2+}}}{dx} \right)_{x=L'} \quad (12)$$

At sites where the OPD and NPD are clearly separated (Sta. EM, CM, SW), the calculated rates and the reaction stoichiometry $1/8 R_{\text{Fe}^{2+} \text{ oxidation}} = R_{\text{NO}_3^-}$ (Table 2) suggest that the DNR coupled to iron oxidation accounts for < 2.2% of the total nitrate consumption (Table 3). At the locations where the OPD, NPD, and the depth of iron oxidation overlap (Fig. 7), the reduced iron is likely oxidized predominantly by O_2 , as oxygen is a more favorable electron acceptor.

Sediment contributions to the nitrogen budget in Lake Superior—The nitrogen budget in Lake Superior has recently attracted attention (Finlay et al. 2007; Sterner et al. 2007; Small et al. 2013), as it appeared imbalanced (Sterner et al. 2007; Li 2011), with inputs of nitrogen

Table 5. The nitrogen budget in Lake Superior. Contributions from this work are in italic; all others are from Sterner et al. (2007). All fluxes and rates are area-specific ($\mu\text{mol m}^{-2} \text{d}^{-1}$); the surface area of Lake Superior is 82,100 km². Positive fluxes are into the sediment.

Source or sink	Contribution to N budget		
	Water column	Sediment	Entire lake
Atmospheric deposition (NO_3^- and NH_4^+)	82		82
Watershed input (NO_3^- , NH_4^+ , and organic N)	90		90
N fixation	Unknown		
Outflow (NO_3^- , NH_4^+ , and organic N)	-78		-78
	Offshore (90% area)	Nearshore (10% area)	Weighted average
Organic N sedimentation	<i>470</i>	<i>650</i>	-490
Organic N burial	<i>54</i>	<i>78</i>	-56
NO_3^- flux at SWI	-270	160	227
NH_4^+ flux at SWI	-45	-27	43
DON flux at SWI		Unknown	Unknown
Removal to N_2 by denitrification and anammox	<i>100</i>	<i>760</i>	-170
Total input			440
Total output			-570
Imbalance			-130

exceeding outputs. Previous studies quantified the total nitrogen inputs into the lake with the direct precipitation, tributary inflows, and outflows (Sterner et al. 2007), but sediment contributions remained unclear (Li 2011). Some of the sediment fluxes were quantified in the coastal regions of the lake, and denitrification rates were estimated (at 0–0.04 $\text{mmol m}^{-2} \text{d}^{-1}$) near the Keweenaw Peninsula (Carlton et al. 1989), but few measurements existed for the offshore regions (Heinen and McManus 2004; Stark 2009). Although recent efforts (Small et al. 2013) provided more information, the contributions to the lake-wide nitrogen budget from processes such as sediment denitrification and anammox, permanent burial of organic nitrogen, and nitrogen exchanges in the potential hotspots of denitrification, such as enclosed bays, remain insufficiently quantified.

Table 5 shows the updated Lake Superior nitrogen budget, which includes our results for the sediment–water exchanges, sedimentary removal of reactive nitrogen to N_2 , and burial of organic nitrogen. The results reveal that, as is the case in the global ocean, where coastal sediments contribute disproportionately to N cycling and removal (Dalsgaard et al. 2005), the N cycle in Lake Superior needs to be considered separately for the areas of high and low sedimentation. Figure 8 compares the deeply oxygenated sediments in low-sedimentation regions, typically offshore, to the typical sediments with shallow OPDs. The disparity in the N_2 production rates indicates that the offshore-type sediments, while covering most of the lake floor (90% as an estimate, actual numbers are unknown), may account for a disproportionately small fraction (46%) of the total benthic nitrogen removal to N_2 . In contrast, the nearshore-type sediments, while representing 10% of the lake floor area, may account for 54% of the nitrogen removal. For comparison, in the Global Ocean the continental margin sediments in < 150 m water depth, while accounting for less than 20% of the ocean floor area, contribute 50% to the benthic N_2 production (Dalsgaard et al. 2005).

Our calculated effluxes of nitrate for the offshore stations (0.19–0.33, average 0.27 $\text{mmol m}^{-2} \text{d}^{-1}$) are higher than the previous estimates in Lake Superior (0.15 $\text{mmol m}^{-2} \text{d}^{-1}$; Heinen and McManus 2004) and significantly higher than the recent estimate of 0.031 $\text{mmol m}^{-2} \text{d}^{-1}$ by Small et al. (2013), who worked closer to shore. For the average nearshore flux of nitrate into the sediments of 0.16 $\text{mmol m}^{-2} \text{d}^{-1}$ (Fig. 8), the lake-average nitrate efflux is into the water column at 0.23 $\text{mmol m}^{-2} \text{d}^{-1}$. The effluxes of ammonium are small at all locations (average 0.042 $\text{mmol m}^{-2} \text{d}^{-1}$). The dissolved organic nitrogen (DON) fluxes are poorly constrained (0.34 \pm 0.31 $\text{mmol m}^{-2} \text{d}^{-1}$ by Stark [2009] and 0.059 \pm 0.173 $\text{mmol m}^{-2} \text{d}^{-1}$ by Small et al. [2013]). In marine sediments, DON fluxes are typically small, less than 5% of the fluxes of inorganic nitrogen (NO_3^- and NH_4^+ ; Devol and Christensen 1993; Burdige and Zheng 1998). Using the DON flux estimates in Lake Superior (Stark 2009; Small et al. 2013), we calculate that the fluxes of inorganic nitrogen (nitrate and ammonium) from the sediments account for 24% to 61% of the total nitrogen inputs into the water column of Lake Superior (Table 5).

The burial of organic nitrogen into the deep offshore sediments is estimated at 0.054 $\text{mmol N m}^{-2} \text{d}^{-1}$, based on the organic carbon burial rate of 0.7 $\text{mmol m}^{-2} \text{d}^{-1}$ (Li et al. 2012) and a 12 C : 1 N stoichiometry (Stark 2009). The burial rate in the nearshore sediments is only slightly higher: 0.078 $\text{mmol N m}^{-2} \text{d}^{-1}$. (This estimate is based on a typical organic carbon content of \sim 1 wt% [Kistner 2013] and a sedimentation rate of 0.06–0.18 $\text{g cm}^{-2} \text{yr}^{-1}$ [Kemp et al. 1978; Evans et al. 1981; Li 2011], which gives the organic carbon burial rate of 0.51–1.52 $\text{mmol m}^{-2} \text{d}^{-1}$.) This yields the average lake-wide burial of nitrogen of \sim 0.056 $\text{mmol m}^{-2} \text{d}^{-1}$. This is comparable to the loss of nitrogen from the lake with the outflow (0.078 $\text{mmol m}^{-2} \text{d}^{-1}$) and corresponds to 33% of the estimated combined inputs of total nitrogen from the atmosphere and watershed (the nitrogen fixation rate is not known; Sterner et al. 2007). The

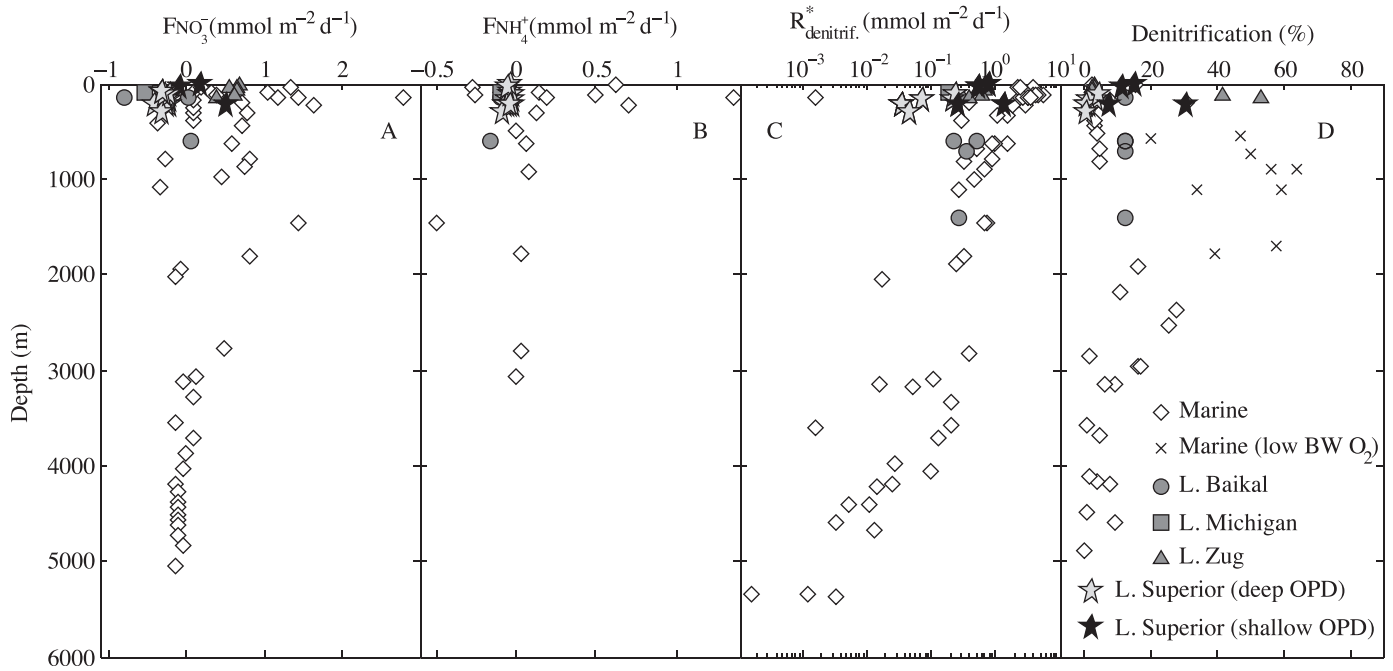


Fig. 9. (A, B) Fluxes of nitrate and ammonium across the SWI, (C) sediment denitrification rates, and (D) percent of deposited organic carbon mineralized by denitrification, organized by water depth. The data are from Lake Superior (this study), Lake Baikal (Maerki et al. 2006), Lake Michigan (Thomsen et al. 2004), Lake Zug (Maerki et al. 2009), and marine sediments (Devol and Christensen 1993; Middelburg et al. 1996; Burdige 2006; Glud et al. 2009). BW O₂, bottom water O₂.

sediment contributions to the total nitrogen budget in Lake Superior are thus significant and need to be considered.

For the water column of the lake, the total nitrogen losses (0.57 mmol m⁻² d⁻¹) exceed the total nitrogen inputs (0.44 mmol m⁻² d⁻¹; Table 5). The difference of 0.13 mmol m⁻² d⁻¹ may be attributable to the uncertainties in the budget numbers; unquantified contributions, such as from nitrogen fixation and DON fluxes; and the existence of non-depositional areas (Kemp et al. 1978). The nitrogen budget for the sediment column appears to be nearly balanced (Fig. 8; Table 5): the present-day net flux of N across the SWI matches the long-term burial flux. The sediments of Lake Superior, being sources of inorganic nitrogen to the water column, are therefore sinks for total nitrogen: they remove nitrogen as N₂ and bury the non-reactive organic N. These two nitrogen sinks account for 73% of the total nitrogen removal in the lake. The total nitrogen losses (0.31 mmol m⁻² d⁻¹) for the entire lake (Table 5) exceed the total nitrogen inputs (0.17 mmol m⁻² d⁻¹). This budget is closer to balance than the previous one (Sterner et al. 2007), in which inputs outweighed losses even without the contribution from nitrogen fixation.

Implications for marine sediments—In marine environments, the sediment nitrogen cycle is often discussed based on water depth, with coastal and abyssal sediments as end members (Middelburg et al. 1996). In water depths similar to those in Lake Superior (0–200 m), marine sediments are typically nitrate sinks, by which nitrate moves from the water column into the sediment (Fig. 9). In Lake Superior this is the case only for the locations with relatively high

sedimentation rates, typically nearshore locations. The rates of nitrogen removal in these sediments are comparable to those in coastal marine environments (Fig. 9), with denitrification accounting for 10–20% of the organic carbon mineralization (Fig. 9; Table 4). The offshore sediments in Lake Superior, however, are more analogous to the oceanic hemipelagic and pelagic sediments than to coastal sediments. Where oxygen penetrates deeply (3 to > 15 cm) and sedimentation rates are low (~0.01 g cm⁻² yr⁻¹;

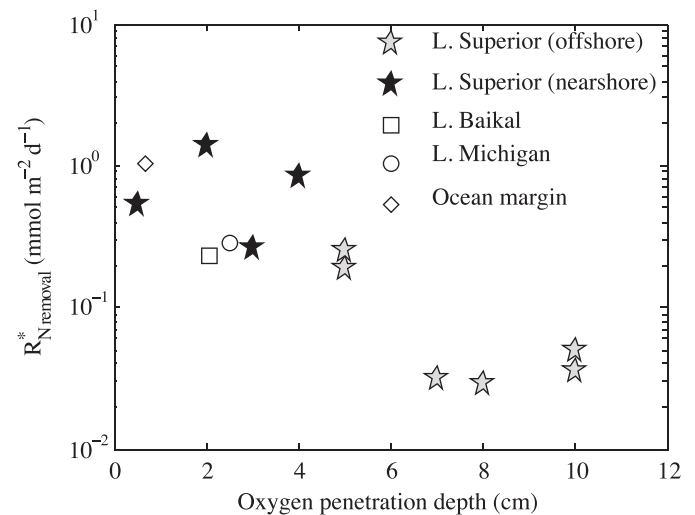


Fig. 10. The rates of reactive nitrogen removal vs. oxygen penetration. The data are from Lake Superior (this study), Lake Baikal (Maerki et al. 2006), Lake Michigan (Thomsen et al. 2004), and ocean margin sediments (Glud et al. 2009).

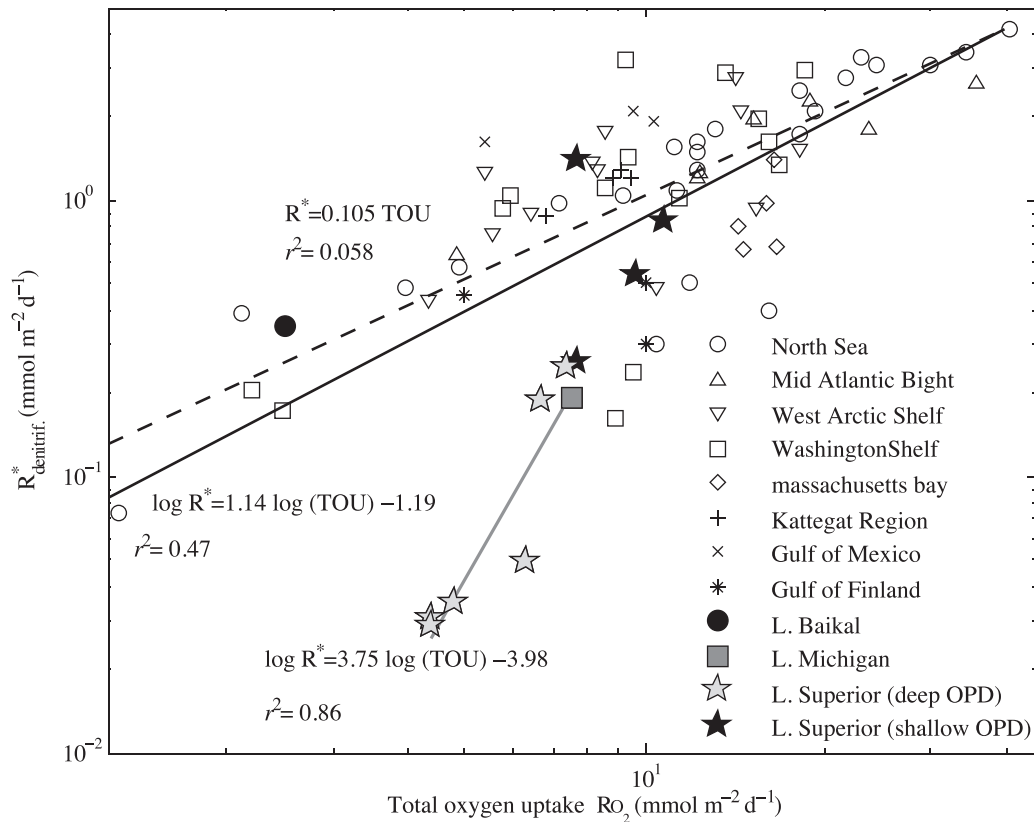


Fig. 11. Denitrification rates vs. sediment oxygen uptake. The data are from Lakes Superior (this study), Baikal (Maerki et al. 2006), and Michigan (Thomsen et al. 2004) and marine sediments (Canfield et al. 1993; Laursen and Seitzinger 2002; Hietanen and Kuparinen 2008; Glud et al. 2009). The lines are the linear model of Laursen and Seitzinger (2002; dashed), the fit to the data from coastal and shelf marine sediments, large lakes (*see* Fig. 10 caption), and the Lake Superior nearshore sediments in this study (solid black) and the fit to the Lake Superior offshore sediments with deep OPDs (solid gray).

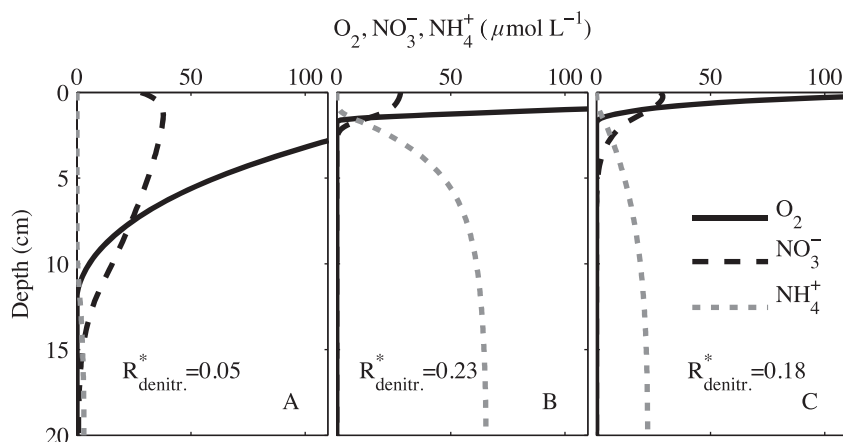


Fig. 12. A diagram illustrating the effect of oxygen penetration on denitrification rates. The vertical concentration profiles of oxygen, nitrate, and ammonium were generated, for illustration purposes, using the diagenetic model LSSE-Mega (Katsev et al. 2007). (A) Conditions typical for the Lake Superior offshore sediments: burial velocity of 0.2 mm yr^{-1} (at 20 cm depth, after compaction); oxygen and nitrate concentrations at the SWI of 350 and $28 \text{ } \mu\text{mol L}^{-1}$, respectively. (B) Same, but the burial velocity is 2 mm yr^{-1} . (C) Same as (A), but oxygen concentration at the SWI is $175 \text{ } \mu\text{mol L}^{-1}$. The depth-integrated denitrification rates, $R^*_{\text{denitr.}}$, are in $\text{mmol m}^{-2} \text{ d}^{-1}$ (compare to Fig. 11). The total sediment oxygen uptake (TOU) is the same in all cases, about $4 \text{ mmol m}^{-2} \text{ d}^{-1}$.

Li et al. 2012), the nitrate effluxes and removal rates (Table 3) are similar to those in the marine sediments in 500–2000 m of water. Denitrification accounts for only < 5% of the organic carbon mineralization (Fig. 9). The effluxes of ammonium in Lake Superior are lower than in marine sediments in similar water depths (Fig. 9) but comparable to those in the deeply oxygenated carbon-poor sediments of the deep ocean (> 3000 m). This suggests that the categorization of sediments based on oxygen penetration (or sedimentation rate, which is a correlated quantity; Li et al. 2012), is more appropriate than the one based on water depth. The importance of oxygen penetration can be seen in other lakes as well: for example, the well-oxygenated sediments in Lake Michigan (OPD > 2 cm; Thomsen et al. 2004) are nitrate sources to the water column and have lower denitrification rates than the shallowly oxygenated sediments in Lake Zug (OPD < 0.2 cm; Maerki et al. 2009) that are nitrate sinks (Fig. 9). Figure 10 shows the negative correlation between the OPD and the rates of nitrogen removal for the sediments of Lakes Superior, Michigan, and Baikal and in the deep continental margins (~ 1,500 m). The rates of nitrogen removal decrease with oxygen penetration, as longer oxygen exposure times leave less reactive carbon for denitrification.

The total oxygen uptake (TOU), a common measure of organic carbon sedimentation (Glud 2008), was previously found to correlate linearly with the denitrification rates in the continental slope and shelf sediments (Fig. 11): $R_{\text{denitrif.}}^* = 0.116 \times \text{TOU}$ ($r = 0.80$; Seitzinger and Giblin 1996) and $R_{\text{denitrif.}}^* = 0.105 \times \text{TOU}$ ($r = 0.76$; Laursen and Seitzinger 2002). The linear relationship is reasonable when denitrification is limited by the supply of nitrate, as nitrification both consumes oxygen and supplies nitrate for denitrification (Laursen and Seitzinger 2002). However, in carbon-poor sediments, our results suggest that the relationship may be stronger than linear (Fig. 11). In addition to being dependent on the supply of nitrate, the denitrification rate is regulated by the amount and reactivity of organic carbon that reaches the denitrification zone. Whereas the carbon amount is reflected in the TOU, the depth of the denitrification zone is linked to the depth of oxygen penetration (Fig. 12), which in deeply oxygenated sediments depends on the rate of carbon sedimentation nonlinearly (Katsev et al. 2006). The combined effect of these factors results in a stronger-than-linear relationship between the TOU and the denitrification rates (Fig. 11). Whereas the nearshore sediments in Lake Superior conform to the same relationship as marine coastal sediments (Fig. 11), the deeply oxygenated sediments are characterized by significantly lower denitrification rates (Fig. 11). Our results (Figs. 11, 12) indicate that the TOU cannot be uniquely correlated to the rates of sediment denitrification. Sediments characterized by the same oxygen uptake (i.e., receiving effectively the same sedimentation flux of organic carbon) may exhibit radically different denitrification rates, depending on the depth of oxygen penetration, which is deeper in slowly accumulating sediments (Fig. 12). This suggests that the deeply oxygenated abyssal sediments in the ocean may not conform to the same relationships as coastal and continental shelf sediments and

need to be treated differently in geochemical models that address the global nitrogen cycle. For the freshwater nitrogen cycle, our results suggest that large oligotrophic lakes generally conform to the trends observed in marine systems, so models from marine environments may be transferable to lakes.

Acknowledgments

We thank Sean Crowe, Matthew Kistner, and David Miklesh for help with sample acquisition and processing; Sean Crowe, Robert Hecky, Maria Dittrich, Robert Sterner, Jacques Finlay, and Gaston Small for discussions; Jay Austin for sharing his National Science Foundation (NSF)-funded cruise opportunities in June and October 2009; Elizabeth Minor, Stephanie Guildford, and Josef Werne for sharing their laboratory facilities; Bogdana Krivogorsky for preliminary analyses of pore waters; and Robert Sterner for recovering the bay core samples for preliminary analyses. We gratefully acknowledge the help of Captain Mike King and the crew of the R/V *Blue Heron*, marine technician Jason Agnich, and laboratory technician Sarah Grosshuesch. The work has been supported by the NSF Ocean Sciences (OCE) grant 0961720, the University of Minnesota–Duluth start-up funds to S.K., the Water Resources Science Block Grant, and University of Minnesota–Duluth Physics Department summer fellowships to J.L. We thank two anonymous reviewers for comments that helped improve the manuscript.

References

- BENZ, M., A. BRUNE, AND B. SCHINK. 1998. Anaerobic and aerobic oxidation of ferrous iron at neutral pH by chemoheterotrophic nitrate-reducing bacteria. *Arch. Microbiol.* **169**: 159–165, doi:10.1007/s002030050555
- BOUDREAU, B. P. 1997. Diagenetic models and their implementation: Modeling transport and reactions in aquatic sediments. Springer.
- BURDIGE, D. J. 1993. The biogeochemistry of manganese and iron reduction in marine sediments. *Earth Sci. Rev.* **35**: 249–284, doi:10.1016/0012-8252(93)90040-E
- . 2006. *Geochemistry of marine sediments*. Princeton Univ. Press.
- , AND S. ZHENG. 1998. The biogeochemical cycling of dissolved organic nitrogen in estuarine sediments. *Limnol. Oceanogr.* **43**: 1796–1813.
- CANFIELD, D. E., AND OTHERS. 1993. Pathways of organic carbon oxidation in three continental margin sediments. *Mar. Geol.* **113**: 27–40, doi:10.1016/0025-3227(93)90147-N
- CARLTON, R. G., G. S. WALKER, M. J. KLUG, AND R. G. WETZEL. 1989. Relative values of oxygen, nitrate, and sulfate to terminal microbial processes in the sediments of Lake Superior. *J. Gt. Lakes Res.* **15**: 133–140, doi:10.1016/S0380-1330(89)71467-2
- CHRISTENSEN, J. P., AND G. T. ROWE. 1984. Nitrification and oxygen consumption in northwest Atlantic deep-sea sediments. *J. Mar. Res.* **42**: 1099–1116, doi:10.1357/002224084788520828
- CODISPOTI, L. A., J. A. BRANDES, J. P. CHRISTENSEN, A. H. DEVOL, S. W. A. NAQVI, H. W. PAERL, AND T. YOSHINARI. 2001. The oceanic fixed nitrogen and nitrous oxide budgets: Moving targets as we enter the anthropocene? *Sci. Mar.* **65**: 85–105.
- COLOWAY, F., AND M. BENDER. 1982. Diagenetic models of interstitial nitrate profiles in deep sea suboxic sediments. *Limnol. Oceanogr.* **27**: 624–638, doi:10.4319/lo.1982.27.4.0624
- DALSGAARD, T., B. THAMDRUP, AND D. CANFIELD. 2005. Anaerobic ammonium oxidation (anammox) in the marine environment. *Res. Microbiol.* **156**: 457–464, doi:10.1016/j.resmic.2005.01.011

- DEVOL, A. H., AND J. P. CHRISTENSEN. 1993. Benthic fluxes and nitrogen cycling in sediments of the continental margin of the eastern North Pacific. *J. Mar. Res.* **51**: 345–372, doi:10.1357/002240933223765
- , L. A. CODISPOTI, AND J. P. CHRISTENSEN. 1997. Summer and winter denitrification rates in western Arctic shelf sediments. *Cont. Shelf Res.* **17**: 1029–1050, doi:10.1016/S0278-4343(97)00003-4
- DICKENS, G. R., M. KOELLING, D. C. SMITH, L. SCHNIEDERS, THE IODP EXPEDITION 302 SCIENTISTS. 2007. Rhizon sampling of pore waters on scientific drilling expeditions: An example from the IODP expedition 302, Arctic Coring Expedition (ACEX). *Scientific Drilling* 4, doi:10.2204/iodp.sd.4.08.2007
- EVANS, J. E., T. C. JOHNSON, E. C. ALEXANDER, JR., R. S. LIVELY, AND S. J. EISENREICH. 1981. Sedimentation rates and depositional processes in Lake Superior from ²¹⁰Pb geochronology. *J. Gt. Lakes Res.* **7**: 299–310, doi:10.1016/S0380-1330(81)72058-6
- FENNEL, K., AND OTHERS. 2009. Modeling denitrification in aquatic sediments. *Biogeochemistry* **93**: 159–178, doi:10.1007/s10533-008-9270-z
- FINLAY, J. C., G. E. SMALL, AND R. W. STERNER. 2013. Human influences on nitrogen removal in Lakes. *Science* **342**: 247, doi:10.1126/science.1242575
- , R. W. STERNER, AND S. KUMAR. 2007. Isotopic evidence for in lake production of accumulating nitrate in Lake Superior. *Ecol. Appl.* **17**: 2323–2332, doi:10.1890/07-0245.1
- GLUD, R. N. 2008. Oxygen dynamics of marine sediments. *Mar. Biol. Res.* **4**: 243–289, doi:10.1080/17451000801888726
- , AND OTHERS. 2009. Nitrogen cycling in a deep ocean margin sediment (Sagami Bay, Japan). *Limnol. Oceanogr.* **54**: 723–734, doi:10.4319/lo.2009.54.3.0723
- GRASSHOFF, K., K. KREMLING, AND M. EHRHARDT [EDS.]. 1999. *Methods of sea water analysis*. Wiley-VCH.
- GUILDFORD, S. J., AND R. E. HECKY. 2000. Total nitrogen, total phosphorus and nutrient limitation in lakes and oceans: Is there a common relationship? *Limnol. Oceanogr.* **45**: 1213–1223, doi:10.4319/lo.2000.45.6.1213
- HEINEN, E. A., AND J. MCMANUS. 2004. Carbon and nutrient cycling at the sediment-water boundary in western Lake Superior. *J. Gt. Lakes Res.* **30**: 113–132, doi:10.1016/S0380-1330(04)70381-0
- HIETANEN, S., AND J. KUPARINEN. 2008. Seasonal and short-term variation in denitrification and anammox at a coastal station on the Gulf of Finland, Baltic Sea. *Hydrobiologia* **596**: 67–77, doi:10.1007/s10750-007-9058-5
- HOLMES, R. M., A. AMINOT, R. KÉROUEL, B. A. HOOKER, AND B. J. PETERSON. 1999. A simple and precise method for measuring ammonium in marine and freshwater ecosystems. *Can. J. Fish. Aquat. Sci.* **56**: 1801–1808.
- HULTH, S., AND OTHERS. 2005. Nitrogen removal in marine environments: Recent findings and future research challenges. *Mar. Chem.* **94**: 125–145, doi:10.1016/j.marchem.2004.07.013
- KATSEV, S., G. CHAILLOU, AND B. SUNDBY. 2007. Effects of progressive oxygen depletion on sediment diagenesis and fluxes: A model for the lower St. Lawrence River Estuary. *Limnol. Oceanogr.* **52**: 2555–2568, doi:10.4319/lo.2007.52.6.2555
- , B. SUNDBY, AND A. MUCCI. 2006. Modeling vertical excursions of the redox boundary in sediments: Application to deep basins of the Arctic Ocean. *Limnol. Oceanogr.* **51**: 1581–1593, doi:10.4319/lo.2006.51.4.1581
- KEMP, A. L. W., C. I. DELL, AND N. S. HARPER. 1978. Sedimentation rates and a sediment budget for Lake Superior. *J. Gt. Lakes Res.* **4**: 276–287, doi:10.1016/S0380-1330(78)72198-2
- KISTNER, M. M. 2013. Organic carbon reactivity in Lake Superior. M.Sc. thesis. Univ. of Minnesota.
- LAURSEN, A. E., AND S. P. SEITZINGER. 2002. The role of denitrification in nitrogen removal and carbon mineralization in Mid-Atlantic Bight sediments. *Cont. Shelf Res.* **22**: 1397–1416, doi:10.1016/S0278-4343(02)00008-0
- LI, J. 2011. Diagenesis and sediment-water exchanges in organic-poor sediments of Lake Superior. M.Sc. thesis. Univ. of Minnesota.
- , S. A. CROWE, D. MIKLESH, M. KISTNER, D. E. CANFIELD, AND S. KATSEV. 2012. Carbon mineralization and oxygen dynamics in sediments with deep oxygen penetration, Lake Superior. *Limnol. Oceanogr.* **57**: 1634–1650, doi:10.4319/lo.2012.57.6.1634
- MAERKI, M., B. MÜLLER, C. DINKEL, AND B. WEHRLI. 2009. Mineralization pathways in lake sediments with different oxygen and organic carbon supply. *Limnol. Oceanogr.* **54**: 428–438, doi:10.4319/lo.2009.54.2.0428
- , ———, AND B. WEHRLI. 2006. Microscale mineralization pathways in surface sediments: A chemical sensor study in Lake Baikal. *Limnol. Oceanogr.* **51**: 1342–1354, doi:10.4319/lo.2006.51.3.1342
- MATISOFF, G., AND X. WANG. 1998. Solute transport in sediments by freshwater infaunal bioirrigators. *Limnol. Oceanogr.* **43**: 1487–1499, doi:10.4319/lo.1998.43.7.1487
- MEILE, C., P. BERG, P. VAN CAPPELLEN, AND K. TUNCAY. 2005. Solute-specific pore water irrigation: Implications for chemical cycling in early diagenesis. *J. Mar. Res.* **63**: 601–621, doi:10.1357/0022240054307885
- MIDDELBURG, J., K. SOETAERT, P. M. J. HERMAN, AND C. H. R. HEIP. 1996. Denitrification in marine sediments: A model study. *Glob. Biogeochem. Cycles* **4**: 661–673, doi:10.1029/96GB02562
- OSTROM, N. E., D. T. LONG, E. M. BELL, AND T. BEALS. 1998. The origin and cycling of particulate and sedimentary organic matter and nitrate in Lake Superior. *Chem. Geol.* **152**: 13–28, doi:10.1016/S0009-2541(98)00093-X
- RYSGAARD, S., N. RISGAARD-PETERSEN, N. P. SLOTH, K. JENSEN, AND L. P. NIELSEN. 1994. Oxygen regulation of nitrification and denitrification in sediments. *Limnol. Oceanogr.* **39**: 1643–1652, doi:10.4319/lo.1994.39.7.1643
- SCHUBERT, C. J., E. DURISCH-KAISER, B. WEHRLI, B. THAMDRUP, P. LAM, AND M. M. M. KUYPERS. 2006. Anaerobic ammonium oxidation in a tropical freshwater system (Lake Tanganyika). *Environ. Microbiol.* **8**: 1857–1863, doi:10.1111/j.1462-2920.2006.01074.x
- SEITZINGER, S. P. 1988. Denitrification in freshwater and coastal marine ecosystems: Ecological and geochemical significance. *Limnol. Oceanogr.* **33**: 702–724, doi:10.4319/lo.1988.33.4_part_2.0702
- , AND A. E. GIBLIN. 1996. Estimating denitrification in North Atlantic continental shelf sediments. *Biogeochemistry* **35**: 235–260, doi:10.1007/BF02179829
- , S. W. NIXON, AND M. E. Q. PILSON. 1984. Denitrification and nitrous oxide production in a coastal marine ecosystem. *Limnol. Oceanogr.* **29**: 73–83, doi:10.4319/lo.1984.29.1.0073
- , AND OTHERS. 2006. Denitrification across landscapes and waterscapes: A synthesis. *Ecol. Appl.* **16**: 2064–2090, doi:10.1890/1051-0761(2006)016[2064:DALAWA]2.0.CO;2
- SMALL, G. E., AND OTHERS. 2013. Rates and controls of nitrification in a large oligotrophic lake. *Limnol. Oceanogr.* **58**: 276–286, doi:10.4319/lo.2013.58.1.0276
- STARK, R. A. 2009. Nitrate production and nitrogen and carbon cycling in Lake Superior sediments. M.Sc. thesis. Univ. of Minnesota.

- STERNER, R. W., T. ANDERSEN, J. J. ELSE, D. O. HESSEN, J. M. HOOD, E. MCCAULEY, AND J. URABE. 2008. Scale-dependent carbon:nitrogen:phosphorus seston stoichiometry in marine and freshwaters. *Limnol. Oceanogr.* **53**: 1169–1180, doi:10.4319/lo.2008.53.3.1169
- , AND OTHERS. 2007. Increasing stoichiometric imbalance in North America's largest lake: Nitrification in Lake Superior. *Geophys. Res. Lett.* **34**: L10406, doi:10.1029/2006GL028861
- STRAUB, K. L., AND B. E. E. BUCHHOLZ-CLEVEN. 1996. Enumeration and detection of anaerobic ferrous iron-oxidizing, nitrate-reducing bacteria from diverse European sediments. *Appl. Environ. Microbiol.* **64**: 4846–4856.
- THOMSEN, U., B. THAMDRUP, D. A. STAHL, AND D. E. CANFIELD. 2004. Pathways of organic oxidation in deep lacustrine sediment, Lake Michigan. *Limnol. Oceanogr.* **46**: 2046–2057, doi:10.4319/lo.2004.49.6.2046
- VIOLLIER, E., P. W. INGLET, K. HUNTER, A. N. ROYCHOUDHURY, AND P. VAN CAPPELLEN. 2000. The ferrozine method revisited: Fe(II)/Fe(III) determination in natural waters. *Appl. Geochem.* **15**: 785–790, doi:10.1016/S0883-2927(99)00097-9
- ZHU, G., AND OTHERS. 2013. Hotspots of anaerobic ammonium oxidation at land-freshwater interfaces. *Nat. Geosci.* **6**: 103–107, doi:10.1038/ngeo1683

Associate editor: Ronnie Nohr Glud

Received: 12 June 2013

Accepted: 22 November 2013

Amended: 25 November 2013